Available online at www.sciencedirect.com
SCIENCE DIRECT®
Journal of Nuclear Materials 355 (2006) 142–149
journal of nuclear materials
www.elsevier.com/locate/jnucmat

Density changes in plutonium observed from accelerated aging using Pu-238 enrichment

B.W. Chung *, S.R. Thompson, C.H. Woods, D.J. Hopkins, W.H. Gourdin, B.B. Ebbinghaus

University of California, Lawrence Livermore National Laboratory, P.O. Box 808, Livermore, CA 94551, United States

Received 11 January 2005; accepted 2 May 2006

Abstract

In support of Stockpile Stewardship activities, accelerated aging tests on a plutonium alloy enriched with 7.3 at.% of ^{238}Pu is underway using dilatometry at 35, 50, and 65 °C and immersion density measurements of materials stored at 50 °C. Changes in density are expected from radiation damage in the lattice and helium in-growth. After 25 equivalent years of aging, the dilatometry data shows that the alloys at 35 °C have expanded in volume by 0.11–0.12% and have started to exhibit a near linear expansion behavior primarily caused by the helium accumulation. The average He-to-vacancy ratio from tested specimens was determined to be around 2.55. The model for the lattice damage and helium in-growth accurately represents the volume swelling at 35 °C. The density converted from the dilatometry corresponds well to the decreasing density trend of reference plutonium alloys as a function of time.

PACS: 61.80.−x; 6182.Bg

1. Introduction

The assessment of aging effects in the plutonium lies at the heart of science-based stockpile stewardship [1,2]. Plutonium, because of its radioactive nature, ages by means of self-irradiation damage and thus produces Frenkel-type defects (vacancies and self-interstitial atoms) and defect clusters. The half-life of the major isotope ^{239}Pu is 24 390 years, and it decays mainly by α-particle decay. Each decay event produces two energetic nuclear particles: a helium nucleus, which receives just above 5 MeV, and a recoil uranium nucleus, which receives about 85 keV [1,2]. The α-particle (helium nucleus) captures two electrons from the plutonium metal to become helium in the lattice, which can associate with crystal defects such as vacancies. In principle, both the uranium and helium decay products can damage the crystal lattice through collisions with plutonium atoms. However, the highly energetic α-particles lose nearly 99.9% of their energy to electrons, thereby heating the plutonium crystal lattice. In contrast, the heavier uranium

* Corresponding author. Tel.: +1 925 4233896; fax: +1 925 4226892.
E-mail address: chung7@llnl.gov (B.W. Chung).

0022-3115/$ - see front matter
doi:10.1016/j.jnucmat.2006.05.015

nuclei convert nearly 75% of their 85 keV of decay energy into the atomic displacements, which cause most of the initial damage to the plutonium lattice. Together, both α-particles and uranium nuclei produce roughly 2500 Frenkel-pairs for each radioactive decay event [1,2]. While most of the initial damage is annealed out at room temperature, the helium formation and residual lattice damage drive microstructural and physical property changes. Radiation damage from alpha decay in plutonium occurs at a rate of ~0.1 dpa (displacement per atom) per year, while the rate of helium production is ~41.1 appm (atomic parts per million) per year [1].

It is well known in the nuclear-energy industry that reactor steels undergo microstructural changes from radiation exposure, which include reduction in density, hardening, and embrittlement [3]. Void swelling, which produces a density decrease, is characterized by three stages [1,3]: an incubation period, a transient period, and a steady-state swelling period. During the incubation period, void nucleation takes place with little or no change in initial density or volume. In general, this period is determined by the time required to accumulate about 5–10 appm of helium. During the transient period, a state of parity is established between the dislocation and void sink strength. This period can extend from a few to 100 dpa, depending on microstructure, temperature, dose rate, and composition. During the steady-state swelling period, the volume swelling rate can accelerate to a value of 1% per dpa for irradiated alloys in reactor environments [3]. This final stage is the consequence of an imbalance or 'bias' of the irradiation-induced vacancies and interstitials to dislocations and voids, respectively. While these general features of swelling are observed in metals and alloys under prolonged exposure at high radiation dose in the appropriate temperature range, they have not yet been observed in naturally aged plutonium alloys [1].

Prior research regarding plutonium aging at ambient temperature is limited. The X-ray diffraction study by Chebotarev and Utkina [4] on Pu alloys aged at room temperature for 2.5 years showed lattice expansion and the lattice parameter reached essentially a constant value in 2–3 years [4]. Positron annihilation measurements indicate that helium-filled vacancies are present in significant numbers in aged plutonium samples [5,6]. Recent transmission electron microscopy investigation of aged Pu–Ga alloys revealed the presence of nanometer-sized helium bubbles formed from helium in-growth [7]. However, most experiments on self-irradiation damage in plutonium (for example, resistivity measurements [2,8,9]) have been conducted at cryogenic temperatures over very short time periods where very little annealing occurs. Such studies do not represent the plutonium aging behavior at ambient temperature.

A preliminary assessment of radiation damage in gallium stabilized δ-plutonium at ambient temperature by Wolfer [1] indicates the void swelling is expected to begin after 10–100 years after fabrication. This estimate is made by assuming that δ-plutonium has radiation and helium effects consistent with typical fcc metals. However, there is no evidence for void swelling in naturally aged plutonium alloys, even after 42 years [7]. Because the effects of interest occur over decades, one approach to better characterize the kinetics of void swelling is to accelerate the effects of self-irradiation damage in plutonium by incorporating a small amount of the more active isotope ^{238}Pu into the ^{239}Pu lattice. The rate of α-decay of ^{238}Pu is nearly 300 times that of ^{239}Pu so the rate of radiation damage accumulation can be increased significantly by adding less than 10 at.% ^{238}Pu. Using this method, the radiation damage in plutonium equivalent to sixty years of natural aging can be simulated in only a few years. However, to achieve equivalent defect structures in an alloy that is enriched in ^{238}Pu, the annealing rate must also be increased by raising the temperature at which aging occurs. In this paper, we report on the initial volume changes observed from in situ dilatometry and immersion density measurements on the 7.3 at.% ^{238}Pu enriched plutonium alloy and reference plutonium alloys of various ages. The immersion density results are used to validate the dilatometry. Because of uncertainties in the proper annealing temperature to balance the accelerated damage, the dilatometry experiments are performed at three different temperatures, i.e., at 35 °C, 50 °C, and 65 °C. Plutonium reference alloys were stored (aged) at 50 °C.

2. Experimental

2.1. Sample preparation and chemical analysis

Pyrochemical processing methods were used to produce both reference and 7.3 at.% ^{238}Pu-enriched plutonium alloys with nominal compositions of

~2 at.% Ga. Details of alloy preparation, which included direct oxide reduction of PuO_2 with Ca, electrorefining, alloying, and casting, are presented elsewhere [10]. Density and dilatometer specimens were machined from the alloys after annealing at ~450 °C for 12 h. Density specimens, each weighing nominally 5 g, were cut into rectangular shapes. Additional density specimens were made from two chemically identical Pu–Ga alloys aged 2.5 years (33 g) and 22 years (1 and 3 g). Dilatometer specimens were 2 mm square by 2 cm or 3 cm long with masses of 1.2 gram and 1.7 gram, respectively.

Isotopic and elemental analyses were obtained from inductively coupled mass spectrometry (ICP-MS) on the enriched alloy. The results of this analysis are compared with the reference alloy in Table 1. The analyses on the individual disks showed very small variations from the values in Table 1, as indicated by the standard deviations. Note that analysis for C, N, and Si could not be conducted by ICP-MS.

2.2. Dilatometry

Specially designed dilatometers were set up inside a nitrogen atmosphere glovebox to monitor long-term growth resulting from the lattice damage and helium in-growth in 7.3 at.% ^{238}Pu-enriched alloys. The schematic of the dilatometer system is presented elsewhere [11], so only a brief description is provided here. Each dilatometer unit consists of a sample vacuum chamber fitted with three linear variable differential transducers (LVDTs). An LVDT measures minute changes, less than 0.02 μm, in the position of a push-rod by monitoring changes in the inductance of a detector coil. In this system, the detector coil is placed outside of the sample chamber. Each dilatometer has a copper sample holder, 3.2 cm in diameter and 2.7 cm high, with three wells: one for a 3 cm long specimen, one for a 2 cm long specimen, and one for a 3 cm long system reference material (Schott glass 'Zerodur', 'zero' expansion glass). Each dilatometer unit can hold two specimens of either circular or square cross-section, 2 or 3 cm long by 2–2.5 mm in diameter. Two different lengths of ^{238}Pu-enriched alloy specimens are used to differentiate between surface effects and volumetric swelling in the materials. Bulk changes are expected to be proportional to the length and any surface effects are expected to be nominally the same between the two samples. Plutonium specimens are placed in the temperature controlled copper sample holder that rests on an ultra-low expansion glass (Schott glass 'Zerodur') inside the sample chamber. This 'Zerodur' provides a stable reference for length measurements, and its position is monitored continuously with one of the three LVDT rods. The other two LVDT rods are placed on the top ends of two plutonium specimens, which protrude from each well. The bottom ends of plutonium specimens rest on the 'Zerodur' reference. Once the specimens and the LVDT rods are positioned, the chamber is sealed with copper gaskets, evacuated with an oil-free vacuum pump and backfilled with high purity helium. The high purity helium, which has high thermal conductivity, minimizes temperature gradients that may result from the specimen extending above the copper sample holder. The glovebox atmosphere is nitrogen, and it is maintained to within ±0.5 °C. The temperature of the dilatometer and its amplifier are maintained to within ±0.1 °C by constant-temperature water circulation system. With the temperature control and use of the 'Zerodur' reference, the stability of the measurement over a 120 day period is better than ±0.10 μm, which is the systematic uncertainty in the measurement.

Table 1
Induction coupled mass spectrometric analysis for reference and enriched alloys

Element	Minimum detection limit	Reference alloy	Enriched alloy	Units
V	9.2	43.9(23)	27.7(5)	appm
Cr	4.5	D	19.9(22)	appm
Fe	42	1729(126)	1702(139)	appm
Ni	4	365(8)	20(8)	appm
Ga	0.002	1.90(0.01)	2.03(0.05)	at.%
Y	0.5	ND	87.3(64)	appm
Ta	0.3	ND	67.6(93)	appm
W	0.3	ND	1.7(0.1)	appm
^{234}U	0.2	3(1)	181(44)	appm
^{235}U	0.2	80(2)	9(2)	appm
^{237}Np	0.2	11(1)	66(1)	appm
^{238}UPu	0.001	0.013(5)	7.29(6)	at.%
^{239}Pu	0.05	91.80(10)	84.84(1)	at.%
^{240}Pu	0.001	5.85(5)	5.41(6)	at.%
^{241}PuAm	0.0001	0.169(5)	0.146(6)	at.%
^{242}Pu	0.0001	0.046(5)	0.055(4)	at.%

Standard deviations are given in parentheses. Elements below the detection limit are denoted as 'D' and 'ND' in the table, respectively.

For the test specimens, three 2 cm and three 3 cm long dilatometer specimens of ^{238}Pu-enriched alloys were heat treated in high purity helium atmosphere for 30 min at 200 °C, and shortly thereafter a pair of each was loaded into the dilatometers. The heat treatment was needed prior to the loading to anneal out the existing lattice damage formed during storage after specimen fabrication. Each system was then maintained at a separate temperature, i.e., at 35 °C, 50 °C, or 65 °C.

2.3. Immersion density

The immersion density equipment closely matches a design used by Bowman et al. [12] and uses about 200 ml of Fluorinert Electronic Liquid FC-43 as the immersion fluid. Prior to a measurement, the system is calibrated using NIST glass (SRM 1827 A) and a tantalum specimen as standards. During the measurement process, dry weights of each specimen are measured to ±0.01 mg, giving a sensitivity of about $\pm 10^{-4}$ g/cm^3 and overall accuracy of about $\pm 10^{-3}$ g/cm^3. Densities of reference plutonium alloys of various ages are measured at ambient temperature. A correction needs to be applied to the measured density to compensate for the effects of convection currents in the immersion fluid generated by the heat from the alpha decay of plutonium. In addition, because the ^{238}Pu-enriched alloys generate significantly more heat compared to the reference specimens, a test sample needs to be left overnight in the immersion bath to allow the temperature of the bath to reach a steady-state condition so that measurements will be reproducible. As an example, a 5 g sample of 7.3 at.% ^{238}Pu-enriched alloy produces 225 mW of power. To correct for the convection current and obtain the actual density, a series of power generating samples were made of tantalum heated with tungsten heating wire, and heat inputs ranging from 0 to 1030 mW were run in the immersion density unit. The offset in density was fit to the following equation:

$$D_{\text{offset}} = 0.06839 \ln[1 + 0.006173Q], \quad (1)$$

where D_{offset} is the offset in density in units of g/cm^3 and Q is the heat input in mW. At 225 mW, a correction of +0.06 g/cm^3 is required to convert the measured density into the actual density. The errors in the reported densities for enriched alloys are less than 0.02 g/cm^3.

3. Results and discussion

3.1. Dilatometry

The volume change (ΔV) normalized with the initial volume (V_0) of each enriched alloy sample at 35 °C, 50 °C, and 65 °C is shown in Fig. 1. The time is represented as an equivalent time (in years equivalent to natural age) calculated by taking the actual measurement time and multiplying by the accelerating factor (e.g. an initial factor of 18.16). To calculate this factor, the α-decay activities of the ^{238}Pu-enriched alloy and the reference alloy are determined using the concentration of isotopes in Table 1. Then the activity of the enrich alloy is normalized to that of the reference alloy to obtain the factor. This accelerating factor will decrease as the material ages due primarily to decreasing concentration of ^{238}Pu in the specimen. Each dilatometer contains a long (3 cm) and short (2 cm) specimen. Since the volume expansion due to self-irradiation damage is assumed isotropic in the bulk of material and is small compared to the total volume, the $\Delta V/V_0$ of the specimen can be obtained with the approximate relation $\Delta V/V_0 \cong 3\Delta L/L_0$ where $\Delta L/L_0$ represents the measured specimen length change (ΔL) normalized with the initial length (L_0). Table 2 shows the specimen length change (ΔL) and the volume expansion for each specimen after 25 equivalent years of aging. As plotted in Fig. 1, all the enriched alloys have increased in volume significantly. There is a trend in $\Delta V/V_0$ curves with the temperature: Samples expanded

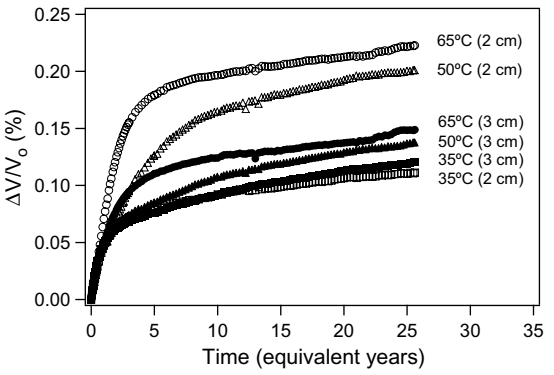

Fig. 1. The normalized volume changes for ^{238}Pu-enriched alloys measured using dilatometry under helium atmosphere at 35, 50, and 65 °C. A pair of 2 and 3 cm length specimens was tested at each temperature. The time is represented as an equivalent aging time calculated by taking the measurement time and multiplying by the accelerating factor.

Table 2
Summary of length change and volume expansion of ^{238}Pu-enriched alloys after 25 equivalent years of aging

Sample temperature (°C)	Sample length (mm, ±0.012)	ΔL (μm, ±0.10)	$\Delta V/V_0$ (%)
35	20.009	7.42	0.11
35	30.009	12.03	0.12
50	20.026	13.40	0.20
50	30.015	13.75	0.14
65	20.023	14.91	0.22
65	30.025	14.89	0.15

more at higher test temperatures. The specimens at 35 °C have expanded in volume by 0.11–0.12% while the 2 cm specimen at 65 °C has expanded by 0.22%. Additionally, the 2 cm length specimens at 65 °C and 50 °C give higher volume change values compared to the 3 cm length specimens. The difference in $\Delta V/V_0$ values for 2 cm and 3 cm length specimens at 50 °C and 65 °C is believed to result mainly from surface effects (i.e. oxidation and/or interfacial reaction with dilatometry components) in the specimens. At 35 °C, both 2 and 3 cm length specimens (open and closed squares in Fig. 1) show similar $\Delta V/V_0$ values indicating minimal surface contribution, and the measured volume change is therefore representative of the bulk material. For comparison, Chebotarev and Utkina [4], using an X-ray diffraction technique, measured lattice expansion of Pu–Ga alloys aged at room temperature for 2.5 years. They extrapolated their results to ~2 at.% Ga and obtained an approximate expansion value of $\Delta a/a_0 \approx 4.5 \times 10^{-4}$ or $\Delta V/V_0 \approx 1.35 \times 10^{-3}$ where a is a lattice constant. This expansion value is between the volume expansion of 65 °C (2 cm) and 65 °C (3 cm) specimens at 2.5 years. Their results show that the lattice parameter of the Pu–Ga alloy increases as a result of prolonged self-irradiation at room temperature. The accumulation of vacancy and self-interstitial lattice defects from the initial cascade damage lead to increase in lattice parameters, which starts to saturate in approximately two to three equivalent years.

3.2. Surface effects and volumetric swelling

The difference in the volume change between 2 and 3 cm length specimens at 50 °C and 65 °C is potentially due to surface effects. If only the bulk swelling accrues from the radiation damage, the dilatometry measurement will show $\Delta L_{(2\,\mathrm{cm})}/L_{0(2\,\mathrm{cm})} = \Delta L_{(3\,\mathrm{cm})}/L_{0(3\,\mathrm{cm})}$ (or $\Delta V_{(2\,\mathrm{cm})}/V_{0(2\,\mathrm{cm})} = \Delta V_{(3\,\mathrm{cm})}/V_{0(3\,\mathrm{cm})}$). However, if the surface effects such as oxidation or interface reaction form significant surface layer, L_s, in addition to the bulk swelling, the fractional length change in the shorter specimen will be larger than the longer specimen, $(\Delta L_{(2\,\mathrm{cm})} + L_s)/L_{0(2\,\mathrm{cm})} > (\Delta L_{(3\,\mathrm{cm})} + L_s)/L_{0(3\,\mathrm{cm})}$. The surface layers, L_s, contribute equally to both specimens since they are made from the same batch of material and tested in the same environment. Thus, the basis for using two different lengths (2 and 3 cm) specimens for the dilatometry is to differentiate between surface effects and volumetric swelling in the specimen.

In a separate experiment, the surface effect on the volume normalization was tested with a surrogate cerium metal (Alfa Aesar, stock no. 10139). Cerium metals are machined to the same specification as the plutonium specimens and tested in the dilatometry under the same conditions. Cerium metal is non-radioactive, and oxidizes rather easily after its surface is polished; it is an ideal candidate for validating surface oxidation effects to dimensional normalization. Fig. 2 shows the 2 and 3 cm length cerium metals held at 50 °C under the helium atmosphere in the dilatometer. The shorter specimen shows larger $\Delta V/V_0$ change compared to the longer sample. This indicates that surface effects such as oxidation can cause the shorter sample to show larger volume changes when normalized to the initial volume as discussed above.

3.3. Physical interpretation of volumetric swelling

During the initial stage of aging at 35 °C in Fig. 1, the volume change follows approximately

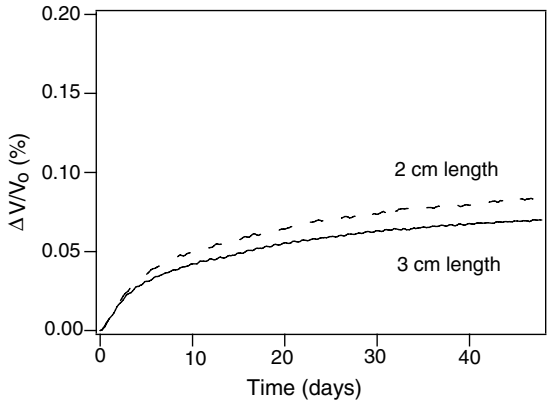

Fig. 2. The normalized volume changes for cerium metals at 50 °C under helium atmosphere. The comparison shows that surface effects such as oxidation cause the shorter sample to show a larger volume change when normalized to the initial volume.

the inverse exponential-type of expansion. This behavior has been observed as an effect of radiation damage in materials [13,14]. The amount of swelling in this case is approximately related to the number of Frenkel pairs that survive the radiation damage and subsequent recombination processes. The progressive accumulation of survivor vacancies provides an increasing number of alternate sites for the capture of self-interstitial plutonium atoms. As the density of these alternate sites increases, the rate of swelling thereby reduced. As discussed above, Chebotarev and Utkina [4] also observed this initial transient stage using X-ray diffraction on plutonium alloys stored for 2–3 years. Based on their results, the initial volume increase is due primarily to an increase in lattice parameter cause by Frenkel defects. This initial stage is observed in the current work up to about 2 equivalent years of aging for samples at 35 °C where the volume expansion becomes reduced. After the initial transient stage, the dilatometry work shows almost linear volume expansion primarily caused by the helium in-growth. The helium that accumulates in plutonium immediately finds unfilled vacancies and forms bubbles inside the crystalline matrix and along grain boundaries [5–7]. The dilatometry shows volume expansion at a steady rate with time primarily induced by a constant helium in-growth rate of ~41.1 appm per year, whereas the data of Chebotarev and Utkina do not [4]. This disagreement is caused by the differences in the measurement techniques. The dilatometry technique measures the changes in the bulk of the material. Thus, it is sensitive to volume (length) changes caused by both the lattice damage and the helium accumulation. Although the X-ray diffraction technique can measure the lattice parameter changes caused by the lattice damage, it is insensitive to the bulk swelling caused by the helium accumulation.

3.4. Volumetric swelling analysis

The dominant contributors to the inverse exponential-type and linear volume swelling are changes in lattice parameters and the build-up of helium, respectively. Thus, the curves at 35 °C are quite accurately represented by the combination of exponential [13,14], linear growth, and small contribution from parabolic surface layer growth equations of the form

$$\Delta V/V_0 \cong A[1-\exp(-Bt)] + Ct + (Dt)^{1/2}, \tag{2}$$

where A is the swelling value at saturation, B is related to the damage volume per time, C is the linear swelling rate by helium accumulation, D is related to surface layer growth rate, and t is the time in years. The constants (A, B, C, and D), as determined from the curve fit, are given in Table 3, along with the He-to-vacancy association ratios and surface layer thicknesses calculated using the slope (C) and (D), respectively. The He-to-vacancy ratio can be approximated with the linear swelling rate and the helium-induced expansion relationship [1]

$$C = (\Delta V/V_0)_{\mathrm{He}}/t \cong [\mathrm{He}]/(R), \tag{3}$$

where $(\Delta V/V_0)_{\mathrm{He}}$ is the helium-induced volume expansion, R represents the He-to-vacancy ratio, and the radiogenic helium concentration [He] is given in atomic parts per million per year. This model describes the linear volume expansion induced by the formation of helium bubbles in the Pu alloy and the average number of helium atoms taking up the volume of a vacancy. The extracted He/vacancy ratios from the equation are 2.74 and 1.91

Table 3
Values of constants from the curve fit (Eq. (2)) to Fig. 1

Sample temperature (°C)	Sample length (mm, ±0.012)	A (10^{-4})	B (year^{-1})	C (10^{-5} year^{-1})	D (10^{-9} m^2 year^{-1})	He/vacancy ratio	L_s (μm)
35	20.009	7.40 ± 0.04	0.88 ± 0.02	1.50 ± 0.03	0.011 ± 0.003	2.74 ± 0.05	0.12 ± 0.01
35	30.009	6.61 ± 0.06	1.17 ± 0.04	2.15 ± 0.02	0.04 ± 0.01	1.91 ± 0.01	0.32 ± 0.03
50	20.026	14.16 ± 0.16	0.30 ± 0.01	1.56 ± 0.08	1.80 ± 0.58	2.64 ± 0.14	2.04 ± 0.16
50	30.015	6.81 ± 0.08	0.83 ± 0.03	1.64 ± 0.08	3.76 ± 0.42	2.51 ± 0.13	2.50 ± 0.21
65	20.023	14.67 ± 0.08	0.65 ± 0.02	1.55 ± 0.05	8.60 ± 0.38	2.64 ± 0.08	3.09 ± 0.69
65	30.025	8.81 ± 0.03	0.73 ± 0.02	1.43 ± 0.03	3.11 ± 0.14	2.87 ± 0.06	2.79 ± 0.62

Eq. (2), however, does not accurately represent dimensional changes at 50 °C and 65 °C due to potential contribution from unresolved physical contributions (see text). He-to-vacancy ratios are calculated from the parameter C and Eq. (3) with the helium production rate of 41.1 appm per year. The surface layer thicknesses are estimated from the parabolic rate constant D. The major contributions to each ratio's error are from the systematic (±0.10 μm) and curve fit uncertainty.

at 35 °C indicating more than one helium atom per vacant lattice site, and the constant C represents the corresponding rate of volume swelling. This ratio should be one if each helium atom captured by bubbles brings with it a vacancy. Thus, helium atoms can fill vacancies and can have an important influence on the subsequent changes in plutonium properties.

The calculated surface layer thickness (L_s) at 35 °C is very small, nearly the systematic uncertainty of the dilatometry measurement. Because of the negligible surface layer thickness, both curves at 35 °C can be also fitted quite accurately with Eq. (2) without the surface layer growth term. Based on the similar $\Delta V/V_0$ values and negligible surface effects, the measured volume change at 35 °C is therefore representative of the bulk material.

Because Eq. (2) represents the model of volumetric swelling and surface layer formation to the volume change, it cannot resolve all the minor competing physical processes (e.g. reactions with dilatometry components) potentially occurring for specimens at 50 and 65 °C. Table 3 includes the constants from the curve fit to 50 °C and 65 °C for comparison to 35 °C. There is a trend in the surface layer thickness (L_s) with the temperature: Samples had thicker surface layers at higher test temperatures. With the exception of the 3 cm length specimen at 50 °C, the constant A is larger and B is smaller than at 35 °C. Furthermore, the constant A for the 2 cm length specimen is significantly larger than the 3 cm length specimen. These discrepancies between the constants A and B are potentially caused by a deficiency in the theoretical model (Eq. (2)) and other unresolved physical processes at higher temperatures. Further investigations are needed to resolve these discrepancies. However, after the initial stage, the contribution from the passivated surface layer (L_s) or other processes to the volume change will be minimal and the linear expansion portion of the volume change curve can be analyzed with the linear growth portion in Eq. (2). The passivated surface layer, estimated to be less than a few microns thick (Table 3) and contributed to the initial volume increase, will have minimal contribution to the volume increase by the helium in-growth. Using this approach, the He-to-vacancy ratio can be extracted with the error primarily originating from the systematic ($\pm$0.10 μm) and curve fit uncertainty. The average ratio from all specimens is about 2.55. This He-to-vacancy ratio represents the helium density within the bubble. At this ratio, it is estimated that the pressure inside the helium bubble is almost off-set by the surface tension of the bubble formed in plutonium [1,15]. If the ratio was larger, between 3 and 4, the significantly greater helium bubble pressure would cause the bubble to grow by dislocation loop punching [15]. At the current ratio, however, the swelling is estimated to substantially less than 0.3% even after 100 years of aging. It is therefore important to examine void swelling mechanisms for any significant future density changes. While this ratio is corroborated by observations from TEM and positron annihilation measurements [5–7], some variations exist between specimens (Table 3). In particular, the 2 and 3 cm length specimens at 35 °C, which represent bulk changes, show different values of 2.74 and 1.91. Whether this large variation is due to a deficiency in the theoretical models (Eqs. (2) and (3)) for analyzing data and computing He-to-vacancy ratio or due to the uncertainty of measurements is unclear at this time. More measurements and more detailed analysis are under way to better quantify the dimensional changes of plutonium alloys during aging.

3.5. Immersion density

In order to compare and validate the accelerated aging method, the immersion density changes in enriched alloys are measured and compared to naturally aged reference plutonium alloys. Comparison of density changes observed in aged reference alloys and ^{238}Pu-enriched alloys to the 35 °C dilatometry data is shown in Fig. 3. The immersion density measurement on the reference and ^{238}Pu-enriched alloys

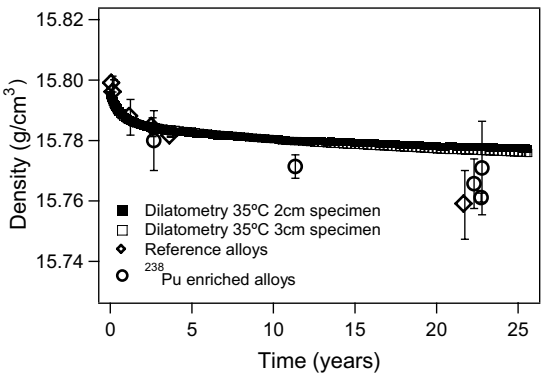

Fig. 3. Comparison of density changes between the enriched alloys from the dilatometry (35 °C) to reference and enriched alloys from the immersion density.

showed initial densities of 15.795 and 15.78 g/cm^3, respectively. The ages of reference samples range from 0.2 to 22 years. Both reference and enriched alloys show reasonable agreement in density changes over time. The dilatometry data was converted to the density using the measured volume change and estimated change in each specimen's mass from radioactive decay. The converted density at time = 0 is set to 15.795 g/cm^3, which is the measured initial reference alloy density, to compare to density changes of the reference alloys. The trend in the density change converted from the dilatometry corresponds well to the immersion density during the initial (exponential) transient stage predominately caused by the lattice damage from the radioactive decay. Following the initial stage, the rate of density reduction becomes reduced as observed from the dilatometry. Both dilatometry and immersion density measurements show dimensional and density changes in enriched Pu alloys induced by the self-irradiation damage. The density changes in Fig. 3 are consistent with the measured volume changes in Table 2. However, no evidence of void swelling is yet observed.

4. Summary and conclusion

We report initial dimensional changes observed from the in situ dilatometry on ^{238}Pu-enriched alloys supplemented by immersion density measurements on both enriched and reference alloys. Dilatometry shows the dimensional expansion from the accumulation of residual lattice damage and helium in-growth. We found reasonable agreement in the density change behavior between enriched and reference alloys from combined dilatometry and immersion density measurements. At 25 equivalent years of aging, there is no evidence of void swelling in any of the materials. Dilatometry measurements show volumetric changes of 0.11% and 0.12% for 2 and 3 cm length samples at 35 °C while showing very slight differences for specimens at higher temperature. Higher temperature measurements are potentially affected by surface effects and/or other unresolved competing physical processes and require further investigation. By modeling the volume swelling measured by the in situ dilatometry, the average He-to-vacancy ratio from tested specimens is estimated to be around 2.55 indicating that the helium bubble pressure is approximately in equilibrium with the surface tension of the bubble formed in plutonium alloy.

Acknowledgements

This work was performed under the auspices of the US Department of Energy by the University of California, Lawrence Livermore National Laboratory under Contract No. W-7405-Eng-48. The authors would like to acknowledge Richard A. Torres and Daniel A. Mew for ICP-MS data.

References

[1] W.G. Wolfer, Los Alamos Sci. 26 (2000) 274.
[2] S.S. Hecker, J.C. Martz, Los Alamos Sci. 26 (2000) 238.
[3] H. Ullmaier, Mater. Res. Soc. Bull. 22 (4) (1997) 14.
[4] N.T. Chebotarev, O.N. Utkina, in: H. Blank, R. Lindner (Eds.), Plutonium and Other Actinides, 1975, Amsterdam, 1976, p. 559.
[5] P.A. Sterne, J. van Ek, R.H. Howell, Comput. Mater. Sci. 10 (1998) 306.
[6] P. Asoka-Kumar, S. Glade, P.A. Sterne, R.H. Howell, in: G.D. Jarvinen (Ed.), Plutonium Futures – The Science, Third Topical Conference on Plutonium and Actinides, Melville, NY, 2003, p. 121.
[7] A.J. Schwartz, M.A. Wall, T.G. Zocco, W.G. Wolfer, Philos. Mag. 85 (2005) 479.
[8] M.J. Fluss, B.D. Wirth, M. Wall, T.E. Felter, M.J. Caturla, A. Kubota, T. Diaz de la Rubia, J. Alloys Comp. 368 (2004) 62.
[9] J.A. Lee, K. Mendelssohn, D.A. Wigley, Phys. Lett. 1 (1962) 325.
[10] K.E. Dodson, O.H. Krikorian, M.S. Blau, W.L. Williams, J.A. Schmitz, D.A. Mew, P.J. Benevento, B.B. Ebbinghaus, Lawrence Livermore National Laboratory Report, UCRL-ID-148262, May 6, 2002.
[11] B.W. Chung, S.R. Thompson, C.H. Conrad, D.J. Hopkins, W.H. Gourdin, B.B. Ebbinghaus, in: L. Soderholm, J.J. Joyce, M.F. Nicol, D.K. Shuh, J.G. Tobin (Eds), Actinides-Basic Science, Applications, and Technology, Mater. Res. Soc. Proc., Pittsburgh, PA, vol. 802, 2003, p. 39.
[12] H.A. Bowman, R.M. Schoonover, M.W. Jones, J. Res. Nat1. Bur. Stand. 71C (1967) 179.
[13] W.J. Weber, J.W. Wald, Hj. Matzke, J. Nucl. Mater. 138 (1986) 196.
[14] W.J. Weber, F.P. Roberts, Nucl. Technol. 60 (1983) 178.
[15] A. Arsenlis, W.G. Wolfer, A.J. Schwartz, J. Nucl. Mater. 336 (2005) 31.